24th COBEM - 2017

24th ABCM International Congress of Mechanical Engineering
December 3-8, 2017, Curitiba, PR, Brazil

COBEM-2017-1173
VIBRATION SUPPRESION OF STRONGLY NONLINEAR STRUCTURE BY MEANS OF NONLINEAR SWITCHING SHUNT CIRCUITS

Tarcisio Marinelli Pereira Silva
Carlos De Marqui Junior
Department of Aeronautical Engineering, Sao Carlos School of Engineering , University of São Paulo, São Carlos, São Paulo, 13566-590, Brazil.
tarcismarinelli@hotmail.com
demarqui@sc.usp.br

Abstract. *This work explores the suppression of undesired saddle-node bifurcations vibrations of geometrically nonlinear structures by using piezoelectric shunt damping circuits, namely the Synchronized Switch Damping on Short-Circuit and the Synchronized Switch Damping on Inductor . The focus is placed on a strongly nonlinear structure that exhibits nonlinear hardening behavior due to a predominantly cubic stiffness. To suppress vibrations associated with saddle-node bifurcations, a purely resistive linear shunting, the SSDS and the SSDI damping techniques are employed and compared with the baseline a short-circuit frequency response curves of the nonlinear structure. Numerical results show that the SSDI scheme substantially reduces the large-amplitude branch and can entirely suppress the bifurcation of the nonlinear system up to certain excitation levels. The numerical results are obtained with a Matlab-Simulink block diagram capable of simulating strongly nonlinear systems (with both mechanical and electrical nonlinearities).*

Keywords: *Vibration reduction, nonlinear structure, nonlinear piezoelectric circuits*

1. INTRODUCTION

Piezoelectric materials convert mechanical energy into electrical energy due to the direct piezoelectric effect. The capability to convert mechanical into electrical energy allows piezoceramic patches to be employed as vibration control devices on a variety of mechanical structures. Especially for lightweight flexible structures, passive piezoelectric control (Lesieutre, 1998 and Ahmadia and Deguilio, 2001) offers remarkable advantages since they are lighter, smaller and easier to be applied than most of the traditional vibration control methods. Passive control using piezoelectric materials started to be studied in the late 1980s and it is still an active field of study nowadays. The investigatins range from experimental beam setups (Hagood and von Flotow, 1991) to aircraft panels (Wu, 2000) and space truss structures (Hagood and Crawley, 1991). A comprehensible review of studies regarding control using piezoelectric materials can be found in Lesieutre (1998) and Ahmadian and Deguilio (2001).

In passive piezoelectric control, piezoelectric material is shunted to simple passive electrical circuits. In this case, the mechanical energy converted into electrical energy (through the direct piezoelectric effect) is dissipated in the electrical domain of the problem. The first applications of passive piezoelectric control reported in the literature are the resistive circuit (Uchino and Ishii, 1988), the inductive shunt circuit (Forward, 1979), the resistive-inductive in series (Hagood and von Flotow, 1991) and the resistive-inductive in parallel (Wu, 1996).

Although the resistive case is compact and easy to implement, the efficiency to reduce vibrations is limited. Capacitive shunting results in a variation of structural stiffness with changing external capacitance. Changing structural stiffness alters the resonance frequencies of the structure and damping is not affected. Resistive-inductive shunting, as reported in the literature by Wu (1996) and Forward (1979), behaves as a damped dynamic vibration absorber effect to the host structure. Although the resistive-inductive (RL) shunt circuits reduce more vibration than the resistive shunt circuits, the required inductances might assume extremely high values in some case, yielding the RL cases to be unviable in practical applications. The inductance of the RL circuits must be tuned according to the target mechanical frequency and piezoelectric capacitance. Since the capacitance of the piezoceramic patch is in the order of nF-uF and if the target mechanical frequency are typically low, the required inductance for RL circuits reach the order of hundreds or even thousands of Henries.

In order to overcome the limited performance of resistive shunts and to overcome the prohibitive high inductances required by the RL shunts, the Synchronized Switching Damping (SSD) techniques have been developed in the early

2000s (Richard et al., 1999, 2000, Clark, 2000, Guyomar et al., 2000 and Corr and Clark, 2002). The SSD techniques are semi-passive or semi-active methods that introduce a nonlinear treatment of the electrical output of piezoelectric elements. The outcome of the nonlinear treatment is a large increase in the mechanical to electrical energy conversion in systems with weak electromechanical coupling. In addition, the nonlinear electrical treatment of the SSD technique results in a phase-agreement between the structural velocity and the piezoelectric voltage output. This way, the energy dissipated by the piezoceramic element is enhanced (when compared to the resistive and the resistive-inductive case), enabling more efficient vibration control.

Nonlinear switching circuits have so far been effectively used for damping of linear resonating structures. In this work, we explore the effectiveness of the SSD circuits for damping of large-amplitude vibrations of a highly nonlinear and electromechanically coupled structure. The nonlinear structure presents hardening behavior in the frequency responses at certain excitation levels due to a predominantly cubic stiffness. The focus of this work is to reduce the large-amplitude response branch in the co-existing response region of the nonlinear structure. The SSD circuits are explored for the possibility of entirely suppressing nonlinear bifurcations of the structure.

2. NONLINEAR STRUCTURE

The nonlinear structure of interest in this work is shown in Figure 1 (from Leadenham and Erturk, 2014, 2015). This structure, named the M-Shaped structure, was originally investigated by Leadenham and Erturk (2014, 2015) for broadband vibration energy harvesting. Here, the same structure platform is used for the application of a SSD circuits. The M-Shaped structure is made of a beam with a width of 25.4mm and thickness of 0.254mm. The beam is made of AISI 1075 spring steel and the bend angles are small enough to allow near zero radius bending without heating the spring. Magnets are attached to the middle of the beam forming a total proof mass of 30.4g. Both ends of the oscillator are clamped, where four piezoceramic patches are attached for providing the electromechanical coupling. Leadenham and Erturk (2014, 2015) used the lumped parameters representation of Figure 1b to model the nonlinear structure. In Figure 1b, k_i and b_a stand for the nonlinear stiffness and the nonlinear aerodynamic damping, respectively. The nonlinear stiffness behavior of the bent beam that causes large-amplitude vibrations is shown in Figure 1d. Aerodynamic damping is included since large amplitude vibrations result in nonlinear dissipative effects (due to air drag, as shown in Bandstra, 1983).

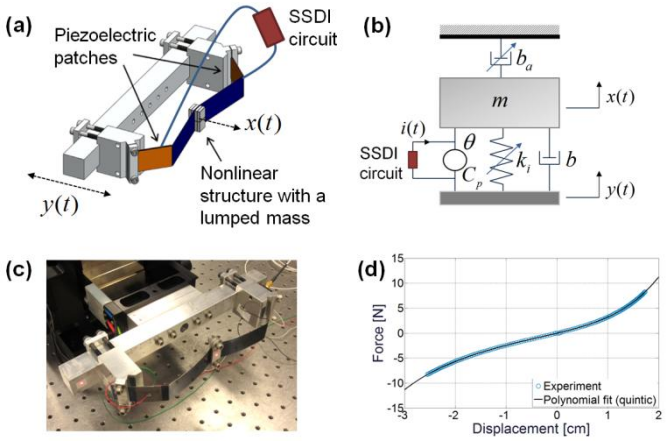

Figure 1. Nonlinear structure explored for bifurcation suppression using nonlinear circuits. a) 3-D model of the nonlinear structure, b) lumped parameters representation, c) experimental structure and d) experimentally measured stiffness behavior with a quintic polynomial fit.

The nonlinear structure is modeled as a single-degree-of-freedom system with linear viscous and quadratic damping terms, a nonlinear elastic restoring force, and linear electromechanical coupling undergoing base excitation.

$$m\ddot{\mathbf{z}} + b_1\left(\dot{\mathbf{y}}+\dot{\mathbf{z}}\right) + b_a\left(\dot{\mathbf{y}}+\dot{\mathbf{z}}\right)\left|\dot{\mathbf{y}}+\dot{\mathbf{z}}\right| + \mathbf{F}_{(\mathbf{z})} - \theta\mathbf{V}_\mathbf{p} = -m^*\ddot{\mathbf{y}} \tag{1}$$

$$\mathbf{F_s(z)} = k_1\mathbf{z} + k_2\mathbf{z}^2 + k_3\mathbf{z}^3 + k_4\mathbf{z}^4 + k_5\mathbf{z}^5 \tag{2}$$

$$C_p\mathbf{V_p} + \mathbf{Q_p} + \theta^t\mathbf{z} = 0 \tag{3}$$

where m is the equivalent mass of the device, m^* is the effective mass due to base excitation, b_1 and b_a are the linear viscous and quadratic damping coefficient, respectively, y is the base displacement, $\mathbf{z}$ is the displacement of the oscillator relative to the moving base, and an overdot represents differentiation with respect to time. C_p is the piezoelectric capacitance, θ is the electromechanical coupling, $\mathbf{Q_p}$ and $\mathbf{V_p}$ are the electrical charge output and piezoelectric voltage output from the piezoelectric material, respectively, and $\mathbf{F_{(z)}}$ is the nonlinear elastic restoring force shown in Eq. 2.

3. LIMITATIONS OF SHUNT DAMPING CIRCUITS

Typical shunt damping circuits frequently reported in the literature are the purely resistive case (originally investigated in Uchino and Ishii, 1988) and the resistive-inductive case (Wu, 1996 and Forward, 1979). When resistive shunts are used, the stiffness of the piezoelectric material continuously increases with the increase of the resistance load while a maximum damping is observed at a specific (optimal) resistor. However, both the stiffness and damping changes are limited. In the case of the M-Shaped structure, the resistive case provided limited suppression of the large amplitude response as shown in Figure 2. In this figure (from Leadenham and Erturk, 2015), the maximum damping provided by the optimal resistive load (R = 300kΩ) results in small shortening of the nonlinear branch. When non-optimal resistance loads are used, less damping is provided and even shorter reductions of the nonlinear branch are observed. Therefore, purely resistive shunts are unlikely to reduce vibration in this strongly nonlinear structure.

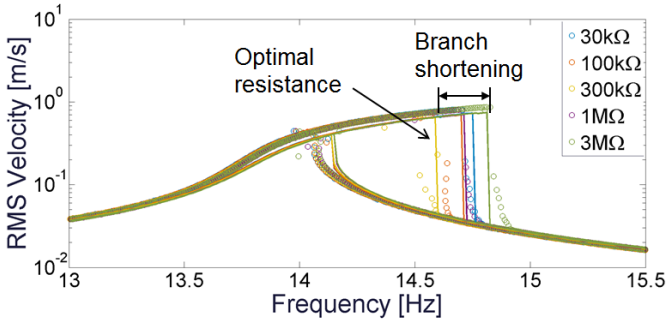

Figure 2. Effect of resistive shunt damping on large-amplitude nonlinear vibration response of the structure. The limited damping increase from resistive shunting results in a very small shortening of the large amplitude nonlinear vibration branch.

An alternative to resistive shunts is the resistive-inductive circuit. In this case, the inductor (L) and the capacitance of the piezoceramic patch must tuned to the target mechanical frequency such that $L = 1/\omega_n^2 C_p$ (where $\omega_n^2 = k_1/m$). Since the target mechanical frequency of the M-Shaped structure is low (lower than 15.5Hz) and the piezoelectric capacitance is in the order of nF, the require inductance of the RL case is above hundreds of Henry. This way, the RL case cannot be employed to reduce vibration in the M-Shaped structure. Therefore in this work, the SSD techniques are employed as an alternative to the RL circuit as discussed in the next section

4. SSD TECHNIQUES

The Synchronized Switching Damping (SSD) techniques were developed in the early 2000s in order to overcome the limitations of the passive techniques (Richard et al., 1999, 2000; Clark, 2000; Guyomar, Richard and Mohammadi et al., 2007; Corr and Clark, 2002). The SSD techniques introduce a nonlinear treatment of the piezoelectric voltage output increasing the mechanical to electrical energy conversion. Furthermore, these techniques impose a phase agreement between the mechanical velocity and the piezoelectric voltage, thus enhancing the shunt-damping effect over passive techniques.

The nonlinear behavior of the SSD technique results from an electrical switch connected to the piezoceramic patch. The electrical switch keeps the piezoceramic patch in the open-circuit condition for most of the time until a voltage extrema (voltage maxima or minina) is detected. When a voltage extrema is detected, the electrical switch connects the piezoeramic patch to the Short-Circuit condition (SSDS) or to an inductor (SSDI). In the SSDS case, a voltage cancelation occurs. In the SSDI case, the capacitance of the piezoceramic patch and the inductor form an oscillating circuit. The switch is kept closed for half a period of the oscillator until the piezoelectric voltage is inverted.

The SSD techniques can be performed with the self powered nonlinear electrical circuit shown in Figure 3. This self powered electrical circuit is composed only by analog components and was originally proposed Richard et al (2007).

Readers are referred to Richard et al (2007) for further details of the circuit. This circuit is one of the most popular self-powered approaches presented in the literature to autonomously detect the voltage extrema.

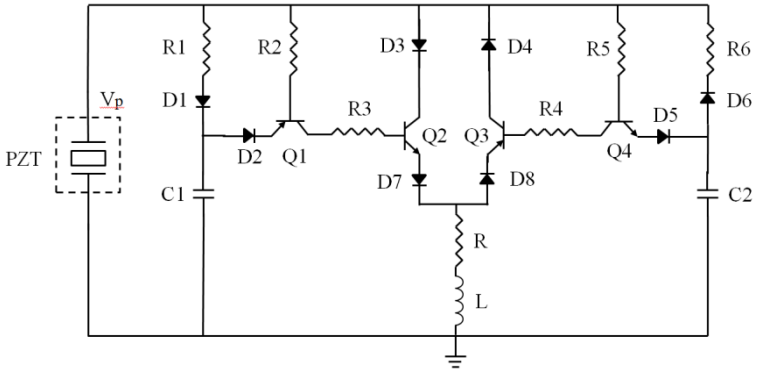

Figure 3: Self-powered nonlinear electrical circuit used to reproduce the SSD techniques.

5. BLOCK DIAGRAM OF THE M-SHAPED STRUCTURE

Leadenham and Erturk (2015) used the harmonic balance (HB) method in order to obtain the steady state solution of the M-Shaped structure. In their paper, the HB method is a reasonable choice since the number of state variables is limited (two mechanical unknowns, $\mathbf{z}$ and $\dot{\mathbf{z}}$, and one electrical variable, $\mathbf{V_p}$). However, when using the SSD techniques, the number of electrical state variables increases considerably (due to the large number of electrical components used in the electrical domain of the problem). With a large number of electrical state variables, the use of the HB method becomes unpractical.

This way, a system-level approach (block diagram) is developed in order to capture the nonlinear behavior of the M-Shaped structure. The Simulink block diagram is shown in Figure 4 and is based on the system-level approach proposed by Elvin (2014). In this system-level approach, Eq. 1 and 3 are rewritten as

$$\ddot{\mathbf{z}} = \frac{1}{m}\left(-b_1\dot{\mathbf{z}} - b_2\left(\dot{\mathbf{y}}+\dot{\mathbf{z}}\right)\left|\dot{\mathbf{y}}+\dot{\mathbf{z}}\right| - \mathbf{F}_{(\mathbf{z})} + \theta\mathbf{V_p} - m^*\ddot{\mathbf{y}}\right) \tag{4}$$

$$V_p = -\frac{\mathbf{Q_p}}{C_p} - \frac{\theta^t\mathbf{z}}{C_p} \tag{5}$$

stating that the inertial term is given as a sum of the linear and nonlinear damping, stiffness, external forces and the electromechanical damping. In addition, Eq. 5 states that the piezoelectric voltage can be modeled as a controlled voltage source ($\theta^t\mathbf{z}/C_p$) connected in series with a capacitor C_p. Equations 4 and 5 are then solved by the block diagram shown in Figure 4 and the problem is solved using the solver ODE15s. In Figure 4, the Electrical Domain block represents the piezoelectric circuit connected to the terminals of the piezoceramic patch. Note that the block diagram is designed to represent the M-Shaped structure regardless of the electrical circuit connected to the piezoceramic patch. This way, the proposed block diagram can be used in vibration control and also energy harvesting problems without any loss of accuracy.

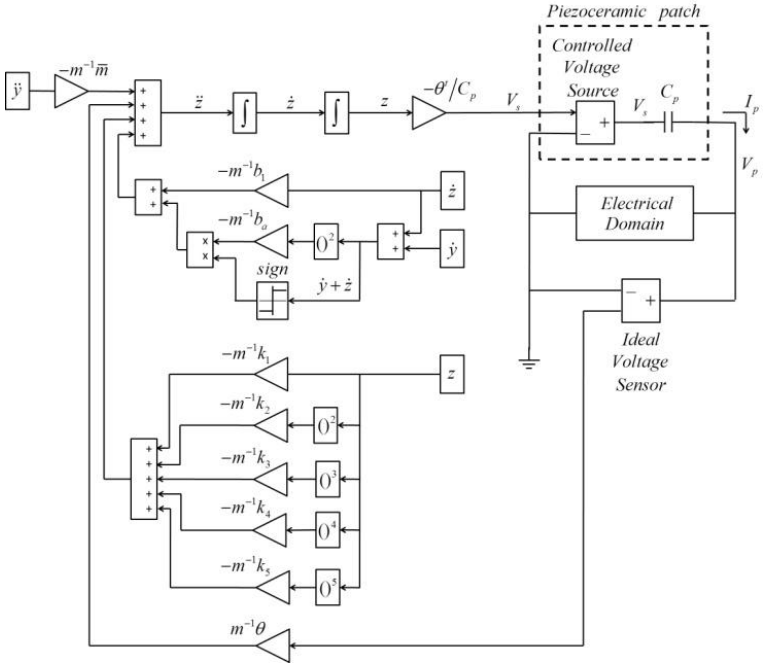

Figure 4: Block diagram used to simulate the nonlinear M-Shaped structure in Matlab-Simulink

6. RESULTS

The goal of this paper is to validate the block diagram model and to analyze the efficiency of the SSD technique to suppress nonlinear vibrations associated with saddle-node bifurcations. To this end, two sections are presented. In the first section, numerical results obtained from the block diagram model are verified against the numerical results provided by Leadenham and Erturk (2015). Leadenham and Erturk (2015) provided mechanical and electrical frequency responses of the M-Shaped structure. In the second section, the block diagram model is used to determine the frequency response curves (up- and down-frequency sweep) of the M-Shaped structure when the piezoceramic patches are connected to the purely resistive linear shunting, SSDS, and SSDI damping techniques. The performance of each piezoelectric circuit (resistive case, SSDS and SSDI) is compared to the baseline (near short-circuit) which, expectedly, shows the largest (and undesired) frequency bandwidth branch to be suppressed.

6.1 Verification of the Matlab-Simulink model

Leadenham and Erturk (2015) empirically identified the mechanical parameters of the M-Shaped structure from experimental tests. The identified parameters are shown in Table 1 and are also used in the system-level model to represent the M-Shaped structure. The natural frequency ($\omega_n^2 = k_1/m$) of the M-Shaped structure is 13.92Hz and, as shown in Leandenham and Erturk (2015), the frequency bandwidth from 13Hz to 15.5Hz is enough to capture the relevant nonlinear behavior of the system. The M-Shaped structure presents a considerably high quality factor of approximately 507.

Table 1. Mechanical parameters of the M-shaped structure.

$m(g)$	$b_1\left(Nsm^{-1}\right)$	$k_1\left(Nm^{-1}\right)$	$\theta\left(NV^{-1}\right)$	$C_p\left(nF\right)$	$k_2\left(Nm^{-2}\right)$
31.9	$5.5\text{x}10^{-3}$	244.1	$170\text{x}10^{-6}$	34.27	2680
$k_3\left(Nm^{-3}\right)$	$k_4\left(Nm^{-4}\right)$	$k_5\left(Nm^{-5}\right)$	$b_2\left(Ns^2m^{-2}\right)$	$\omega_n\left(Hz\right)$	ξ
$363\text{x}10^{3}$	$10.6\text{x}10^{6}$	$210\text{x}10^{6}$	0.012	13.92	0.0010

Figure 5 shows the numerical results presented by Leadenham and Erturk (2015). In this figure, the nonlinear frequency responses of the M-Shaped structure are obtained through controlled up and down frequency sweeps to capture the jump phenomenon associated with saddle-node bifurcation. The frequency sweeps are conducted at a RMS (root mean square) base accelerations level of 0.04g and the excitation frequencies range from 13Hz to 15.5Hz. A frequency step of 0.05Hz is employed and each excitation frequency excites the system for 60s (to ensure that the system reaches the steady state condition). Five different load resistance (30kΩ, 100kΩ, 300kΩ, 1MΩ and 3MΩ) are

considered in the electrical domain of the problem and the RMS mechanical absolute velocity ($\dot{\mathbf{y}}+\dot{\mathbf{z}}$) and the RMS piezoelectric voltage for each resistance load are shown in Figure 5a and Figure 5b, respectively. In Figure 5, the HB solution obtained by Leadenham and Erturk (2015) is represented by the continuous dashed red curves and the solution from the block diagram is represented by the continuous blue curves. The same set of five resistors (30kΩ, 100kΩ, 300kΩ, 1MΩ and 3MΩ) is used in the Electrical Domain block of Figure 4. In both Figure 5a (RMS velocity) and Figure 5b (RMS piezoelectric voltage), the equivalent representation is in good agreement with the HB solution. The main discrepancy is that the block diagram resulted in slightly shorter lengths of the large amplitude response for most of the resistors considered. In the next section, the block diagram is used to obtain the nonlinear frequency response of the M-Shaped structure when the SSD circuits are considered.

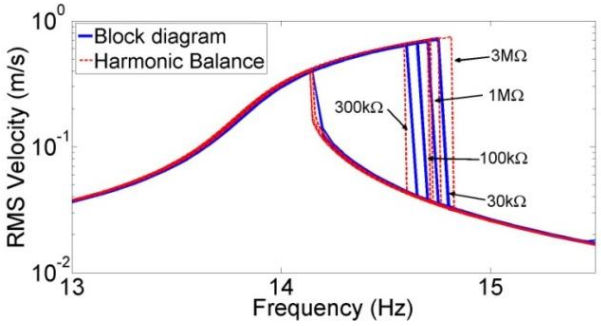

a)

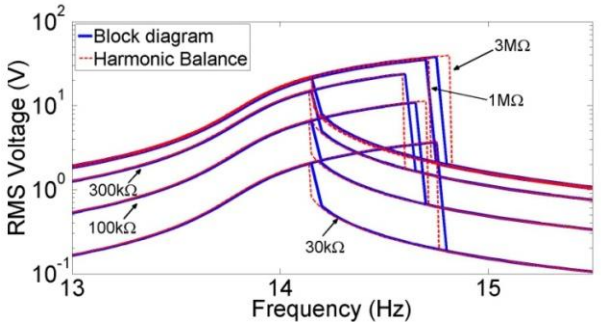

b)

Figure 5. Validation of the equivalent block diagram (used to represent the M-Shapes structure) against the numerical results from Leadenham and Erturk (2015). Good agreement is seen for both the a) absolute mechanical velocity ($\dot{\mathbf{y}}+\dot{\mathbf{z}}$) and b) the piezoelectric voltage.

6.2 M-Shaped structure with the SSD techniques

In this section, the SSD circuits are employed to reduce vibrations of the large-amplitude response branch. The SSD circuit of Figure 3 is used in the Electrical Domain block of Figure 4 and Simulations using the block diagram are performed. The electrical components used to simulate the SSD circuit are shown in Table 2. In the SSD circuit, the electrical components R_1 and C_1 form a low pass filter. The low pass filter plays an important hole for the proper operation of the SSD technique. Since the system is highly nonlinear (with mechanical and electrical nonlinearities), the M-Shaped structure presents considerable oscillations due to higher harmonics. The higher harmonics creates several local extrema in the voltage of the piezoceramic patch. If the electrical switch closes at every local extrema, the efficiency of the SSD technique decreases substantially. The principle of the low pass filter is to allow the SSD technique to ignore local voltage extrema and close the switch only at the global extrema of the piezoelectric voltage. The low pass filter formed by R_1 and C_1 form a time constant given by $\tau = R_1 C_1$. By increasing τ, the cut-off frequency of the low pass filter decreases and the effect of the higher harmonics is attenuated.

Table 2. Mechanical parameters of the M-shaped structure

R_1 and R_6	R_2 to R_5	C_1 and C_2	Diodes D_1 to D_8
10MΩ	1kΩ	6.8nF	BWY95C
Q_1 and Q_3	Q_2 and Q_4	R	L
MPSA92	MPSA42	1702Ω	5H

Figure 6 shows a comparison of the frequency responses of the M-Shaped structure when the resistive, SSDS and the SSDI circuits are considered. In Figure 6a, the RMS mechanical absolute velocity ($\dot{\mathbf{y}} + \dot{\mathbf{z}}$) is presented and in Figure 6b, the RMS piezoelectric voltage is displayed. The same RMS base acceleration of 0.04g, frequency range from 13.0Hz to 15.5Hz and frequency step of 0.05Hz (with a time window of 60s for each frequency) of the previous section are maintained. The baseline case near short-circuit condition (R = 30kΩ) expectedly shows the largest (and undesired) frequency bandwidth branch to be suppressed. The optimal electrical load for the linear resistive load case (extracted from Figure 2) results in a small shortening of the branch, while and as noted earlier, the linear resistive-inductive loading case is impractical in the present configuration (due to extremely large inductance requirements). It is observed that the SSDS circuit offers larger damping and branch shortening than the purely resistive case. However, overall the largest reduction in the large-amplitude branch and almost entire complete suppression of the saddle-node bifurcations of the structure is due to the SSDI circuit.

The SSD technique outperforms the resistive case due to two main reasons. First, the SSD techniques cause a phase agreement between the mechanical velocity and the voltage output of the piezoceramic patch. Consequently, the shunt damping effect is enhanced and the vibration attenuation is increased. Secondly, the voltage output in the SSD technique increase considerably when compared to the resistive case, as shown in Figure 6b. The maximum voltage output of the resistive case is 23.95V while the SSD technique boosts the maximum voltage output to 50.7V (in the SSDS case) and to 102.7V (in the SSDI case). In percentage terms, the self-powered SSDI technique increased in 328% the voltage output of the resistive case.

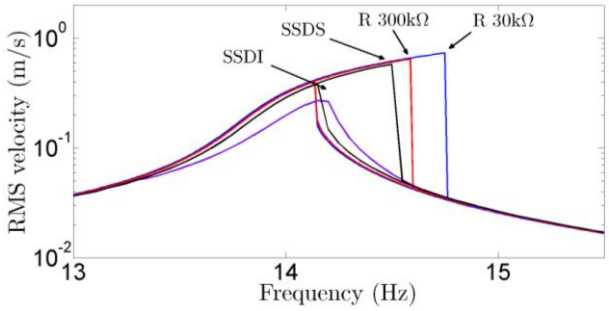

a)

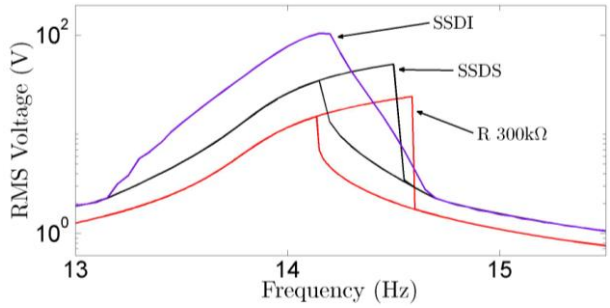

b)

Figure 6. Frequency response of the a) absolute velocity and the b) piezoelectric voltage output of the M-Shaped structure in the frequency range of 13.0Hz to 15.5Hz obtained from the Matlab-Simulink block diagram.

7. CONCLUSIONS

This paper investigates the vibration suppression of a strongly nonlinear flexible structure (named M-Shaped structure) shunted to nonlinear synchronized switch damping techniques. The M-Shaped structure presents extremely low damping and, for this reason, undergoes large mechanical displacements at low excitation levels (below 0.1g). The large mechanical displacements yield the structure to behave nonlinearly. In the lumped parameters model proposed by Leadenham and Erturk (2015) to model the M-Shaped structure, a quintic polynomial stiffness term and a nonlinear quadratic damping term are required to properly predict the mechanical displacements of the system. The cubic stiffness term predominates in the quintic polynomial stiffness. Thereafter, the M-Shaped structure exhibits a nonlinear hardening behavior.

The attenuation of vibration in the M-Shaped structure is performed by passive and semi-passive piezoelectric shunt damping circuits. The use of linear shunt circuits, such as the resistive and resistive-inductive shunts, is discussed in this paper. The resistive shunt modifies the system's stiffness and damping according to the value of the resistance load.

Nonetheless, the stiffness and damping provided by the resistive shunt is limited and are unlikely to reduce a significant amount of vibration in this strongly nonlinear structure. The resistive-inductive shunts reduce more vibration than the resistive shunts. However, in the M-Shaped structure case, extremely high inductances (oh hundreds of Henry) are required.

In order to overcome the limitations of passive techniques, the synchronized switch damping techniques are employed. The SSD imposes a nonlinear treatment of the piezoelectric voltage that increases the mechanical to electrical energy conversion (thus improving the shunt damping effect) and also requires a much lower inductor (5H) than the resistive-inductive shunts. It is observed that the performance of the SSDS circuit is slightly better than the resistive shunts. However, the largest vibration reduction in the large-amplitude branch and almost complete suppression of the saddle-node bifurcations of the structure is due to the SSDI circuit. The SSDI circuit substantially reduces the large-amplitude branch, offering the possibility of entirely suppressing bifurcations of the nonlinear system up to certain excitation levels.

8. ACKNOWLEDGEMENTS

The authors gratefully acknowledge the support of CAPES (99999.003755/2015-00) for funding this project. The authors also gratefully acknowledge the support of CNPq (402160/2013-4) for funding this project.

9. REFERENCES

Ahmadian, M. and Deguilio, A.P., 2001. “Recent advances in the use of piezoceramics for vibration suppression”. *The Shock and Vibration Digest*, Vol. 33, No. 1, pp. 15-22. ISSN 0583-1024. doi: 10.1177/058310240103300102.

Bandstra, J. P., 1983. “Comparison of equivalent viscous damping and nonlinear damping in discrete and continuous vibrating systems”. *Journal of Vibration, Acoustics, Stress, and Reliability in Design*, Vol. 105, No. 3, p. 382. ISSN 07393717. doi: 10.1115/1.3269117.

Clark, W. W., 2000. “Vibration Control with State-Switched Piezoelectric Materials”. *Journal of Intelligent Material Systems and Structures*, Vol. 11, No. 4, pp. 263–271. ISSN 1045389X. doi: 10.1106/18CE-77K4-DYMG-RKBB.

Corr, L.R. and Clark, W.W., 2002. “Comparison of low-frequency piezoelectric switching shunt techniques for structural damping”. *Smart Materials and Structures*, Vol. 11, No. 3, p. 307. ISSN 09641726. doi: 10.1088/0964-1726/11/3/307.

Elvin, N. G., 2014. "Equivalent electrical circuits for advanced energy harvesting". *Journal of Intelligent Material Systems and Structures*, Vol. 25, No. 14, pp. 1715-1726. ISSN 1045-389X. doi: 10.1177/1045389X14521878.

Forward, R.L., 1979. “Electronic damping of vibrations in optical structures”. *Applied optics*, Vol. 18, No. 5, p. 690. ISSN 0003-6935. doi: 10.1364/AO.18.000690.

Guyomar, D., Richard, C., Gehin, C. and Audigier, D., 2000. “Low consumption damping of planar structures”. *IEEE International Symposium on Applications of Ferroelectrics*, Vol. 2, pp. 761–764. doi: 10.1109/ISAF.2000.942431.

Hagood, N.W. and A. von Flotow, 1991. “Damping of structural vibrations with piezoelectric materials and passive electrical networks”. *Journal of Sound and Vibration*, Vol. 146, No. 2, pp. 243-268. ISSN 0022460X. doi: 10.1016/0022-460X(91)90762-9.

Hagood, N.W. and Crawley, E.F., 1991. “Experimental investigation into passive damping enhancement for space structures”. *Journal of guidance, control, and dynamics*. Vol. 14, No. 6, pp. 1100-1109. ISSN 0731-5090. doi: 10.2514/3.20763.

Leadenham, S., and Erturk, A., 2014. "M-shaped asymmetric nonlinear oscillator for broadband vibration energy harvesting: Harmonic balance analysis and experimental validation". *Journal of Sound and Vibration*, Vol. 333. No. 23, pp. 6209-6223. ISSN 0022460X. doi: 10.1016/j.jsv.2014.06.046.

Leadenham, S., and Erturk, A., 2015, "Nonlinear M-shaped broadband piezoelectric energy harvester for very low base accelerations: primary and secondary resonances". *Smart Materials and Structures*, Vol. 24, No. 5, p. 55021. ISSN 1361-665X. doi: 10.1088/0964-1726/24/5/055021.

Lesieutre, G.A., 1998. “Vibration damping and control using shunted piezoelectric materials”. *The Shock and Vibration Digest*. Vol. 30, No. 3, pp. 187-195. ISSN 0583-1024. doi: 10.1177/058310249803000301.

Richard, C., Guyomar, D., and Lefeuvre, E., 2007. “Self-powered electronic breaker with automatic switching by detecting maxima or minima of potential difference between its power electrodes”, WO Patent, Patent PCT/FR2005/003000, Publication number: WO/2007/063194.

Richard, C., Guyomar, D., Audigier, D. and Bassaler, H., Laboratoire, I., Electrique, D. G. and Ferroélectricité, C., 2000. “Enhanced semi passive damping using continuous switching of a piezoelectric device on an inductor”, *SPIE* Vol. 3989, pp. 288–299. doi: 10.1117/12.384569.

Richard, C., Guyomar, D., Audigier, D. and Ching, G., 1999. “Semi-passive damping using continuous switching of a piezoelectric device”. In *Proceedings of SPIE - The International Society for Optical Engineering* (eds VV Varadan, NM Wereley, RO Claus et al), Vol. 3672, p. 104–111.

Uchino, K. and T. Ishii, 1988. "Mechanical damper using piezoelectric ceramics". Journal of the Ceramic Society of Japan, Vol. 96, No. 1116, pp. 863-867. ISSN 1882-1022. doi: 10.2109/jcersj.96.863.

Wu, S. y., 1996. "Piezoelectric shunts with a parallel R-L circuit for structural damping and vibration control". *Symposium on Smart Structures and Materials*. International Society for Optics and Photonics.

Wu, S., Turner, T.L. and Rizzi, S.A., 2000. "Piezoelectric shunt vibration damping of an F-15 panel under high-acoustic excitation". in *SPIE's 7th Annual International Symposium on Smart Structures and Materials*. International Society for Optics and Photonics. Newport Beach, CA, United States.

10. RESPONSIBILITY NOTICE

The authors are the only responsible for the printed material included in this paper.